15

Ultrafast Studies of the Light-Induced Spin Change in Fe(II)-Polypyridine Complexes

Majed Chergui

Ecole Polytechnique Fédérale de Lausanne, Laboratoire de Spectroscopie Ultrarapide (LSU), Switzerland

15.1 Introduction

The phenomenon of spin-crossover (SCO), which implies a thermally induced transition from a low spin (LS) ground state to a high spin (HS) excited state (or the reverse) in metal-based molecular complexes has been demonstrated for derivatives of ions with d^4, d^5, d^6 and d^7 configurations and is observed for all these in complexes of the first transition series.[1] SCO processes can also be triggered by pressure or irradiation by visible light. Research on the latter phenomenon witnessed a major development after McGarvey *et al.*[2, 3] discovered that for a number of iron(II) and iron(III) polypyridine complexes in solution, the HS state could be populated efficiently at the expense of the LS state by pulsed laser excitation. Near ambient temperatures these light-induced HS states have lifetimes ranging from nanoseconds to microseconds, which are governed by the HS to LS relaxation kinetics. Following this discovery, Decurtins *et al.*[4] showed that at cryogenic temperatures the HS/LS relaxation slows down such that under continuous irradiation, the iron(II) spin-crossover systems can be trapped in the HS state, for which the expression 'light-induced excited state spin trapping (LIESST)' was coined. The discovery of LIESST triggered several years of intense research not only with regard to the mechanism of trapping in the HS state of the system but also into the chemical and physical parameters governing the lifetimes of the low temperature metastable HS states.[5, 6] The fact that LIESST can be observed in crystalline solids raised interest in the study of cooperative effects. The interest in spin trapping is not just academic but is also stirred by the potential applications in optical writing/magnetic reading for magnetic data storage.[7, 8] Iron(II) polypyridine complexes are also considered as potential (and cheaper) candidates for dye-sensitized solar cells,[9–12] which have thus far been most successful with ruthenium-based complexes.[13] Finally, Fe(II) polypyridine complexes appear to have several photophysical properties in common with iron porphyrins, which play an important role in respiration and oxygen transport.

Spin-Crossover Materials: Properties and Applications, First Edition. Edited by Malcolm A. Halcrow.

Several studies have been carried out to characterize the spectroscopic, magnetic, structural and dynamic properties of Fe(II) complexes with different ligands, with the aim of identifying the parameters that are crucial to efficient SCO and LIESST switching. In particular, the aim was to identify what controls the lifetime of the lowest excited quintet state, which differs by several orders of magnitude depending on the nature of the ligand, and to identify the route leading from the initial excited state to the lowest quintet state in the SCO process. These studies were nicely reviewed in two volumes published in 2004 that were dedicated to SCO complexes.[1] Since then, there has been an upsurge of ultrafast studies aimed at describing in detail the mechanisms whereby the excited singlet states populates the quintet state on ultrashort timescales.[14, 15] In parallel, several time-resolved structural studies using X-ray diffraction[16–19] and X-ray absorption spectroscopy[15, 20–25] were carried out, aimed at getting information about the electronic and molecular structure of the short lived excited quintet state, or the intermediates leading to it from the initial excited singlet state. Finally, this intense experimental activity has been accompanied by several new theoretical studies that deliver insight into the energetics and the couplings between excited states.[26–32]

Previously, steady-state spectroscopic and X-ray studies on SCO complexes showed several electronic and structural properties common to nearly all Fe(II) complexes.[33–35] This is of importance as properties that are determined for one complex could, to a certain extent, be generalized to the rest of the family of iron(II)-based complexes. The present chapter deals with studies of isolated Fe(II) complexes, mostly in solution. Understanding of the photoinduced dynamics in isolated complexes is of importance for the description of the SCO in crystals, where it is more likely to find applications. In particular, there has been some discussion about the photoswitching of spin of entire domains in such crystals,[19, 36, 37] and it is therefore crucial to understand what occurs at the molecular level. Excellent reviews have appeared that present the results of steady-state and time-resolved spectroscopic studies of the SCO process.[6, 14, 38] This chapter focuses on the recent developments based on novel ultrafast optical and X-ray techniques which have led to new insight into the ultrafast SCO phenomenon.

15.2 Properties of Fe(II) Complexes

We first recall a number of properties that are common to all Fe(II)-based SCO complexes.

15.2.1 Electronic Structure

Iron(II) consists of six electrons in the 3*d* shell. In perfectly octahedral O_h coordination, the five *nd* orbitals of a transition metal ion are split into a subset of three orbitals, namely d_{xy}, d_{yz} and d_{zx}, which are the basis of the irreducible representation t_{2g}, and a subset of two orbitals, namely d_{z^2} and $d_{x^2-y^2}$, which are the basis of the irreducible representation e_g (see Fig. 15.1a). The t_{2g} orbitals are basically nonbonding and are therefore at lower energy than the antibonding e_g orbitals. The splitting between the two sets is referred to as ligand field splitting and is symbolized by the parameter of the ligand field strength. The latter depends upon both the particular set of ligands and the given metal ion. Because the spin-crossover involves transferring electrons from the t_{2g} subshell to the e_g subshell, the Fe–N bond length increases as a result.

Figure 15.1b shows the potential energy level diagram of $[Fe(bpy)_3]^{2+}$ along the Fe–N coordinate.[30] The $^1A_1(t_{2g}{}^6)$ low spin ground state, the lowest excited $^5T_2(t_{2g}{}^4e_g{}^2)$ high spin electronic state, as well as the higher excited singlet, triplet and quintet ligand-field (LF, also called metal-centred, MC) states are shown. In addition, the manifold of low lying singlet and triplet metal–ligand charge transfer (MLCT) states for ligands with extended π-systems is shown as a shaded region. This diagram can be generalized to the family of Fe(II) polypyridine molecular complexes, in terms of the ordering of states but not their absolute energies. This can be gathered from the absorption spectra of the various complexes,[6] and from quantum-chemical calculations

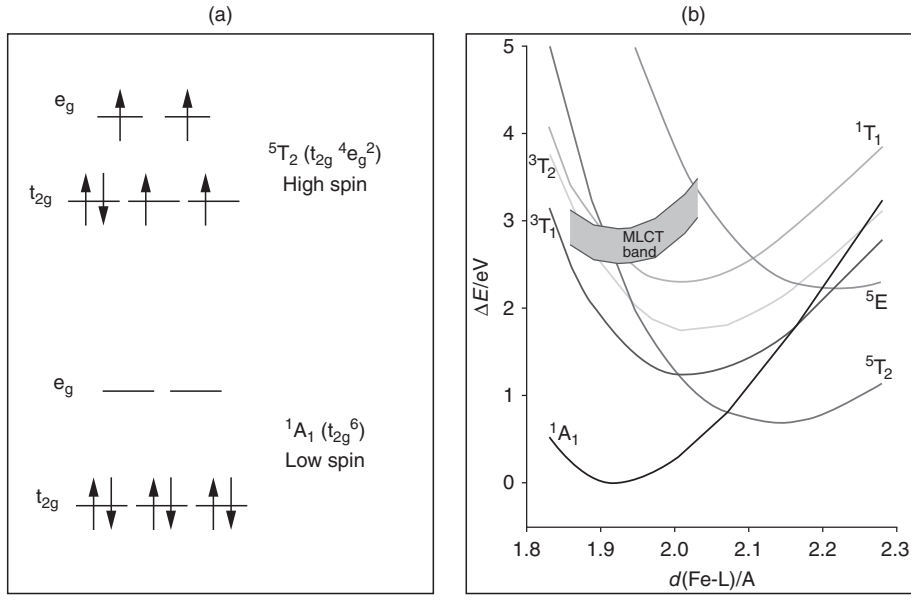

Figure 15.1 *(a) Occupancy of the ligand-field split* d*-orbitals in the low and high spin states; (b) potential curves of [Fe(bpy)$_3$]$^{2+}$ as a function of the Fe-ligand coordinate. The manifold of metal-to-ligand charge transfer (MLCT) states is shown as a grey shaded area. Reprinted with permission from [30]. Copyright 2011 WILEY-VCH Verlag GmbH & Co. KGaA.*

on complexes such as [Fe(bpy)$_3$]$^{2+}$,[27, 30, 31, 39] [Fe(ptz)$_6$]$^{2+}$ (ptz = 1-propyltetrazole),[26] [Fe(tz)$_6$]$^{2+}$ (tz = 1*H*-tetrazole),[28] and [Fe(pap)$_2$]$^+$ (pap = *N*-2-pyridylmethylidene-2-hydroxyphenylaminato).[40]

15.2.2 Molecular Structure

Per electron that is promoted from the t_{2g} to the e_g orbital, the metal–ligand bond length increases by as much as 0.1 Å.[41] In the low spin $^1A_1(t_{2g}^6)$ state, the bond length is centred at 1.96 ± 0.04 Å. In the high spin $^5T_2(t_{2g}^4e_g^2)$ state, the bond length increases by 0.20 Å typically.[28–31, 39] Obviously these parameters change somewhat for different ligand types. They have been determined by static X-ray diffraction and X-ray absorption spectroscopy studies of complexes on the LS state and on the metastable quintet states.[34, 42, 43] We will later see that the same structural change from LS to HS is also verified for systems having short-lived HS, so that the bond length increase is not the parameter that determines the HS lifetime.

For the series of states $^{1,3}T_{1,2}(t_{2g}^5e_g^1)$, the bond length is expected to be intermediate between the LS and HS state, and for the $^5E(t_{2g}^3e_g^3)$ state it is expected to be larger than that of the $^5T_2$ state, as confirmed by quantum-chemical calculations.[27–31, 39] In the case of the $^{1,3}T$ states, their similar bond distances are also corroborated to a certain extent by the width of the absorption bands from the ground state to these states, which are observed at low temperatures.[6]

15.2.3 Vibrational Modes

Another property that is common to all Fe(II)-based complexes is their Fe–N bond stretch frequency, which lies around 390–430 cm^{-1} in the LS state and around 210–250 cm^{-1} in the HS state,[33, 44] supporting the idea of a softer potential due to the more antibonding character in the HS state.

15.2.4 Kinetics of Ground State Recovery

The conversion from the HS quintet state to the LS ground state has been investigated in detail by several groups using steady state spectroscopy of low temperature crystals, and these studies have been reviewed in detail by Hauser in ref. 6. The HS to LS state relaxation was interpreted invoking a multiphonon relaxation in an energy gap law kinetics.

Time-resolved studies of the light-induced SCO started in the 1980s using picosecond and sub-picosecond laser techniques.[6, 14, 38, 45–50] Most of these studies, which concentrated on the determination of the LS ground state recovery in over 10 different Fe(II) polypyridine complexes, are nicely reviewed in ref. 38. It was found that the lowest excited (HS) quintet state relaxes nonradiatively to the LS ground state with times ranging from ∼0.65 ns to ∼150 ns in room temperature solutions.[35] This was established by correlating the timescale of the ground state bleach recovery with the decay time of the quintet excited state absorption, which was found to lie in the 300 nm region.[6, 48, 51]

While the LS ground state recovery seems a well understood process, that leading from the initial excited state to the lowest quintet state has raised several questions regarding the nonradiative cascade leading to the population of the HS state. Here we mainly concentrate on this cascade and on the structural changes occurring in the HS state.

15.3 From the Singlet to the Quintet State

We concentrate on the excitation into the manifold of singlet metal-to-ligand-charge-transfer (^{1}MLCT) states, which act as doorway states to the $\Delta S = 2$ spin change. Based on ideas from organic physical chemistry, initial models describing the photophysics of SCO tended towards the picture that the intermediate $^1T_1$, $^3T_2$ and $^3T_1$ MC states (Fig. 15.1) mediate the relaxation process in $\Delta S = 1$ steps. Vibrational relaxation should then occur on the timescale of the relevant vibrations of the molecule (typically picoseconds), while the electronic processes involved in the SCO are internal conversion (IC) and intersystem crossing (ISC), with the former being much faster than the latter, due to its conservation of spin angular momentum.

However, several results showed that this picture may not be valid in the case of metal-complexes, and in particular Fe(II) ones. Back in the early 1980s, Sutin and co-workers[45] and Netzel and co-workers[52] published a picosecond time-resolved absorption study of the excited-state dynamics of $[Fe(bpy)_3]^{2+}$ in which they reported a unity quantum yield for formation of the lowest energy HS excited $^5T_2$ state following ^{1}MLCT excitation. This was later supported by a study by Hauser, who reported a near unity quantum efficiency for $[Fe(2\text{-pic})_3]^{2+}$ in the solid state at 11 K.[6, 53]

These unity quantum yields are difficult to reconcile with the picture of a relaxation cascade via the intermediate $^1T_1$, $^3T_2$ and $^3T_1$ states, since these are expected to have significant electronic coupling to the ground state. Moreover, in the case of the singlet states, relaxation back to the ground state should be more favourable than cascading towards higher spin states. Furthermore, as mentioned in Section 15.2.4, return to the ground state proceeds exclusively through the $^5T_2$ state. One reason to nevertheless invoke the intermediate state is based on Hauser's low temperature single-crystal study of the spectroscopy of $[Fe(ptz)_6]^{2+}$,[54] where he observed the formation of the $^5T_2$ state with near unity quantum yield following excitation into all four MC states (i.e. $^1T_2$, $^1T_1$, $^3T_2$ and $^3T_1$).

Coming back to time-resolved studies, Hendrickson and co-workers carried out sub-picosecond transient absorption studies of $[Fe(tpen)]^{2+}$ in solution. Although they could not observe a spectroscopic signature of the quintet state, they concluded that it would be formed within the time resolution of the experiment (<700 fs).[47, 48] Similar results were found for several other LS Fe(II) complexes, including $[Fe(bpy)_3]^{2+}$,

suggesting that such ultrafast formation of the $^5T_2$ state is a general feature of the photophysics of Fe(II) polypyridine complexes.

These initial studies were complemented by McCusker and co-workers using $[Fe(tren(py)_3)]^{2+}$ (tren(py)$_3$ = tris(2-pyridylmethyliminoethyl)amine),[10] where they were able to resolve dynamic spectral shifts associated with the formation of the HS state, which would be formed in ∼300 fs. They also observed additional dynamics attributed to vibrational relaxation in the $^5T_2$ state with a time constant of 8 ± 2 ps. Information concerning dynamics associated with the initially formed MLCT state was also unravelled by monitoring spectral changes in regions where the difference spectra for the MC and MLCT states are of opposite sign. They thus concluded that depopulation of the MLCT manifold occurs in 80 ± 20 fs.

The model that was proposed to explain these observations invoked a distinct kinetic process corresponding to conversion from the MLCT to MC manifolds. Beyond that, the model ruled out any intermediate electronic state other than $^5T_2$ as being involved in the photoinduced SCO for Fe(II) complexes. In this picture there is extensive mixing among all of the excited ligand-field (MC) states that lie between the ^{1}MLCT and $^5T_2$ states. However, the picture of the relaxation within the ligand-field manifold was not so clear and it was suggested that it may probably involve a 'barrier less potential slope in which the wave function continuously evolves in its character from something approximating a singlet to that of the $^5T_2$ state'.[38] The problem with the latter idea is that the MC states seem to be parallel to each other, in the sense that they all have the same equilibrium distance and probably the same curvature along the Fe–N coordinate.[6, 27, 28, 30] It also does not explain why the preference would be to feed population into the quintet state at the expense of the ground state. In order to clearly address the issue of the conversion from the MLCT states to the HS states, it is necessary to have means to probe the departure, the intermediate steps (if any) and the arrival of population into the quintet state. Over the past few years there has been an upsurge of studies in ultrafast spectroscopies that aim at specifically addressing this issue.

15.3.1 Departing from the MCLT Manifold

Contrary to their ruthenium analogues, Fe(II)-polypyridine complexes do not exhibit a long lived ^{3}MLCT phosphorescence, due to the fact that the ligand-field states lie at lower energies than the MLCT states.

Broadband femtosecond fluorescence up-conversion was first used on the study of $[Ru(bpy)_3]^{2+}$ by the Lausanne group who could observe both the very short lived ^{1}MLCT for the first time but also the long lived ^{3}MLCT.[55] Decay of the ^{1}MLCT fluorescence (≤30 fs) was reflected in the rise of the ^{3}MLCT emission. The ability to observe the ultrafast depopulation of the ^{1}MLCT by fluorescence up-conversion prompted the same group to investigate the case of $[Fe(bpy)_3]^{2+}$. Figure 15.2a shows a typical 2D time-energy plot of the fluorescence of aqueous $[Fe(bpy)_3]^{2+}$ upon excitation at 400 nm.[56] The time-dependent emission spectra, shown in Figure 15.2b, are obtained by taking slices at fixed time delay, while cuts at fixed emission wavelength provide the kinetic traces shown in Figure 15.2c. Strikingly (and just as for all Ru complexes[55, 57]), the emission centred around 600 nm is already visible at $t = 0$ with a mirror-image like profile with respect to the absorption band (here, in the 500–650 nm region). This behaviour was recently reinvestigated, and showed no dependence on the pump wavelength.[57] The ultrafast relaxation processes occurring in the manifold of ^{1}MLCT states that lead to a mirror-like image (with respect to the absorption band) fluorescence were estimated to occur in <10 fs and were attributed to intramolecular vibrational redistribution (IVR) and internal conversion (IC) processes. The fluorescence appears cold with respect to the high frequency modes of the molecules (which show up as a progression in the absorption band).

Coming back to Figure 15.2a, a weak emission is observed at $\lambda \geq 650$ nm and $t \geq 100$ fs. This observation is confirmed in Figure 15.2b, where the spectrum at $t = 100$ fs exhibits two weak bands of almost identical intensity, the remnant of the fluorescence centred at ∼600 nm, the other at ∼660 nm. Just as for $[Ru(bpy)_3]^{2+}$,[55]

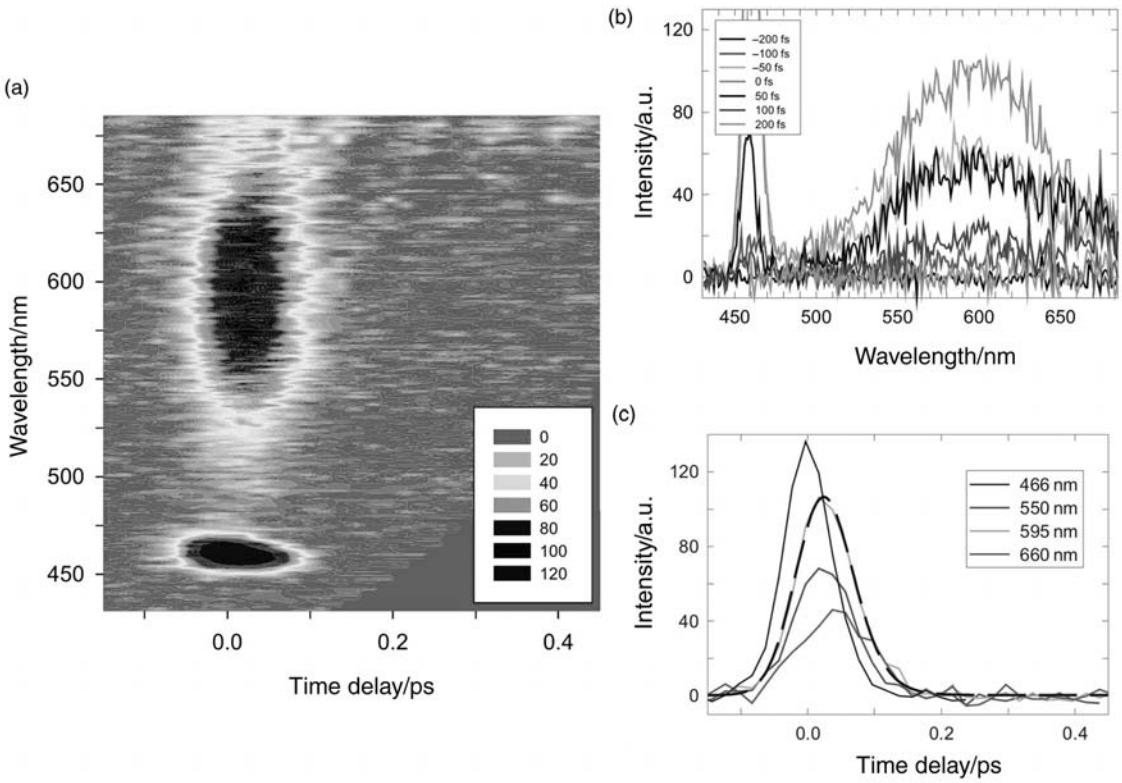

Figure 15.2 *(a) Two-dimensional plot of the femtosecond fluorescence spectra of aqueous $[Fe(bpy)_3]^{2+}$ upon excitation at 400 nm. The signal at 466 nm corresponds to a Raman line of H_2O. (b) Fluorescence spectra at different time delays. (c) Time traces at different wavelengths. Time delays are taken with respect to the water Raman line. The trace at 595 nm is shown together with its fit function. Reprinted with permission from [56]. Copyright 2008, American Chemical Society.*

the comparison of Raman and emission time traces allow us to extract an exponential decay of 30 ± 10 fs for the ^{1}MLCT fluorescence. The weaker emission at ∼660 nm was found to decay in ∼130 fs and is assigned to the ^{3}MLCT state. Indeed, it lies in the wavelength range where the ^{3}MLCT phosphorescence is expected to occur. These results represent the first observation of fluorescence and phosphorescence of Fe(II) SCO complexes. Interestingly, the decay of the ^{3}MLCT state in $[Fe(bpy)_3]^{2+}$ is comparable to the value of 80 ± 20 fs reported for $[Fe(tren(py)_3)]^{2+}$.[10]

The decay of the ^{3}MLCT state of $[Fe(bpy)_3]^{2+}$ was confirmed by transient absorption measurements. Figure 15.3a shows representative spectra recorded at various time delays within the initial 2 ps after photoexcitation. A short-lived excited state absorption (positive signal) appears in the 340–440 nm region, while in the 560–640 nm range it is present even at longer time delays. The former is a clear signature of the MLCT state, since it corresponds to the absorption of the reduced bpy ligand, as established from spectroelectrochemical studies of Fe(II) polypyridine complexes,[58] and from studies of $[Ru(bpy)_3]^{2+}$ whose ^{3}MLCT state is long-lived.[59] In <200 fs, the short wavelength (< 400 nm) excited state absorption is replaced by a negative signal, which we identify as the ground state bleach (GSB) signal, caused by depletion of the ground state due to the photoexcitation by the pump pulse. This bleach signal is dominant in the 450–550 nm spectral range

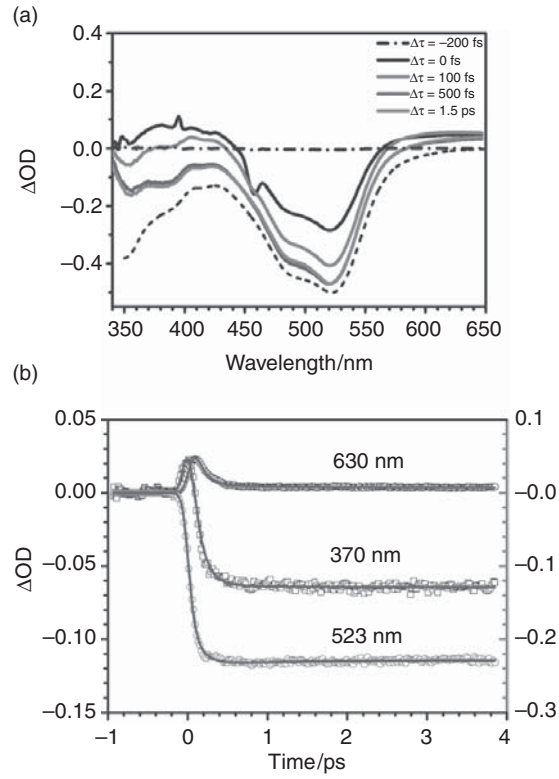

Figure 15.3 *(a) Transient absorption spectra of aqueous $[Fe(bpy)_3]^{2+}$ upon 400 nm excitation. The spectral evolution in the first 1.5 ps after photoexcitation (t = 0) is shown. The peak around 400 nm at t = 0 is the residual scattered light contribution from the pump pulse. The strong negative absorption feature present in the early spectra around 450–460 nm is the impulsively-induced Raman signal of H_2O. The inverted ground state absorption spectrum is displayed (dashed line) for comparison. (b) Kinetic traces of aqueous $[Fe(bpy)_3]^{2+}$ in a 5 ps time window at three selected wavelengths, together with their fit functions using a global fit model (see ref. 56 for details). Reprinted with permission from [56]. Copyright 2008, American Chemical Society.*

and it fully reflects the ground state absorption. Kinetic traces at three characteristic wavelengths (370 nm, 523 nm and 630 nm) are shown in Figure 15.3b. It can be seen that the positive absorption signals at 370 and 630 nm appear within the experimental temporal resolution of 140 fs but behave differently, as already noted in Figure 15.3a. The 630 nm trace is due to the strong absorption of aqueous electrons, which are produced in small quantities by multiphoton excitation, as established from pump power dependence studies.[60] The analysis and modelling of these TA data[56] delivers three global time constants: 115 ± 10 fs, 960 ± 100 fs and 665 ± 35 ps, that fit simultaneously all the kinetic traces in the spectral range of interest. The shortest component reflects the lifetime of the ^{3}MLCT state, in agreement with the above fluorescence up-conversion measurements, while the longest component reflects the ground state recovery by the decay of the $^5T_2$ state. The intermediate component could not be assigned to any given photoinduced species in a straightforward way, and is either due to the solvated electron or to a 1 ps component of the relaxation within the quintet state, which will be presented below. Finally, neither information about a channel via the intermediate $^{1,3}T$ states, nor about the arrival in the quintet states, could be retrieved from these data, either because these states

are spectroscopically silent in the region of our probe wavelength range and/or they are not populated in the subsequent nonradiative cascade.

15.3.2 Arrival into the HS State

Of all the ligand-field states lying lower than the MLCT manifold, the $^5T_2$ state is the only one for which an excited state absorption was known. Hendrickson and co-workers showed that for the complexes $[Fe(tpen)]^{2+}$ and $[Fe(tptn)]^{2+}$, a quintet absorption occurs below 330 nm.[61] The same was established by Hauser in his studies of the absorption spectrum of low temperature crystals of $[Fe(ptz)_6]^{2+}$ entirely photoconverted to the high spin state.[6] Another lower energy absorption band was reported by both groups[6, 62] in the 800–900 nm region but is very weak ($\varepsilon = 5\ \mathrm{lmol^{-1}cm^{-1}}$), and was attributed to the $^5T_2$–^5E transition between MC states. Finally the UV HS absorption also shows up in complexes that have a high spin ground state, such as $[Fe(tren(6\text{-}CH_3\text{-}py)_3)]^{2+}$.[51]

Smeigh *et al.*[51] probed the formation of the HS state upon photoexcitation of the ^{1}MLCT state of $[Fe(tren(py)_3)]^{2+}$ complex in acetonitrile by recording its UV absorption in the region of 285 to 325 nm. From these results, they estimated that the ^5T state is populated in $<$250 fs, which was their time resolution. They complemented this result by fs stimulated Raman scattering studies where, by following the CN stretch frequency of the ligand as a function of time, they deduced a population time of the HS state of 190 $\pm$ 50 fs, alongside a vibrational relaxation of 10 $\pm$ 3 ps within the HS state.

The Lausanne group carried out transient absorption studies of aqueous $[Fe(bpy)_3]^{2+}$ using a white light continuum in the UV, with a cross-correlation of 100 fs.[63] Figure 15.4 shows a representative selection of UV TA spectra at different time delays. The positive region between 300 nm and ~330 nm corresponds to an excited state absorption (ESA), while elsewhere in the spectrum a bleach signal is dominant, which matches quite well the ground state absorption spectrum above 350 nm (see Fig. 15.3). The ESA is due to the quintet state, as evidenced by its decay time of 650–700 ps (see bottom inset, Fig. 15.4), but the kinetics also exhibits a short component of 2–3 ps. By normalizing the absorption spectrum to the TA spectrum above 350 nm, which consists only of the ground state bleach (GSB) signal, we could retrieve the absorption spectrum of

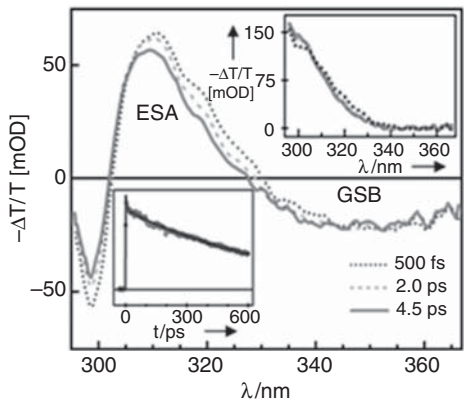

Figure 15.4 *UV transient absorption spectra at different time delays upon excitation of aqueous $[Fe(bpy)_3]^{2+}$ at 530 nm. The lower inset shows a long-time kinetic trace recorded at 315 nm. The upper inset shows the excited state absorption spectra at different time delays, obtained by subtracting the ground state spectrum from the transient spectra. Reprinted with permission from [63]. Copyright 2008 WILEY-VCH Verlag GmbH & Co. KGaA.*

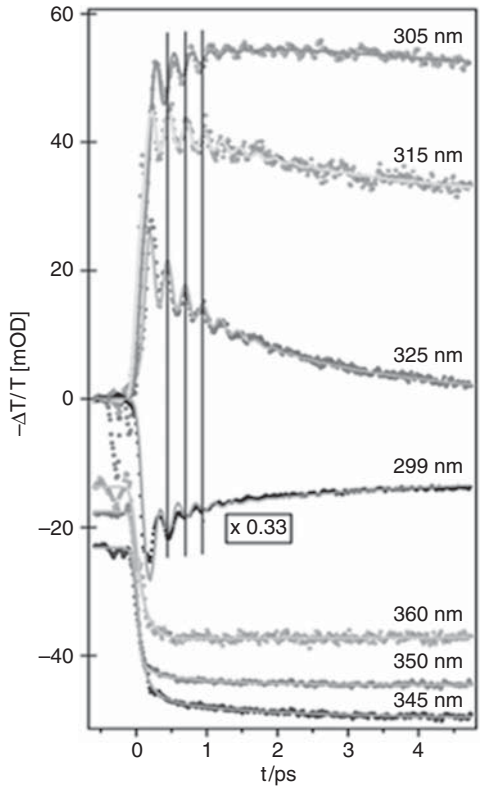

Figure 15.5 *Kinetic traces at different probe wavelengths covering the ESA (305, 315 and 325 nm) and the bleach regions (299, 345, 350 and 360 nm). Solid lines represent the fits with a bimodal relaxation kinetics and an oscillatory contribution. The vertical lines show the phase shift of ∼π of the oscillations between the blue-most and the red-most probe wavelengths in the ESA region. For clarity, time-traces at λ > 340 nm have been vertically shifted and the 299 nm one is scaled to $^1/_3$. Reprinted with permission from [63]. Copyright 2008 WILEY-VCH Verlag GmbH & Co. KGaA.*

the quintet state at different time delays (top inset, Fig. 15.4). The retrieved spectra agree well with those of stable and metastable HS Fe(II) complexes.[6, 47, 49, 51]

Kinetic traces between 300 to 360 nm over the first 5 ps are shown in Figure 15.5. The traces in the ESA region are all characterized by a fast rise followed by an oscillatory pattern and a longer decaying component. The oscillations at the blue and red edges of the ESA (300 and 325 nm) exhibit a phase shift close to π (vertical lines), which is typical of a vibrational wave packet oscillating between the turning points of the potential surface on which it evolves. These traces were analysed in detail in ref. 63, with the experimental data described in terms of MLCT ESA and ground state bleach (GSB) contributions being instantaneously excited and decaying with 130 fs and 650 ps, respectively, while the quintet state ESA rises in 130 fs. Bimodal dynamics with 1.1 ± 0.17 ps and 3.4 ± 1.2 ps time-constants were necessary to obtain optimal fits at short times, along with an oscillatory pattern with a period of 254 ± 2 fs, independent of probe wavelength. However, its damping constants varied between ∼400 to ∼800 fs, depending on the probe wavelength. The results show good agreement with the experimental traces over the whole spectral range (Fig. 15.5). The 1.1 and 3.4 ps components describe a narrowing of the quintet state absorption band due to vibrational cooling, as actually evidenced by increase of its maximum and the presence of an isobestic point around 305 nm

(Fig. 15.4, top inset). The 1.1 ps component may well be associated with the 0.96 ps component derived from the global fit of the visible TA data (Fig. 15.3), in which case the latter cannot be due to the solvated electron.

A vibrational wave packet occurs on the HS surface because it only appears in the region of the ESA region, and is missing in the GSB traces above 325 nm and in the visible region.[56] The reaction coordinate of the photoexcited LS–HS spin change is the Fe–N bond stretch (Fig. 15.1), whose vibrational frequency is ∼220 cm^{-1} (∼150 fs) in the HS state. Hence, the observed wave packet is not directly excited by the laser pump pulse, but by the ultrafast elongation of the Fe–N bonds, which excites bending modes due an impulsive change of N–Fe–N angle. Based on DFT calculations[64] we attribute the observed oscillation to a combination of chelate ring modes, benzene cycle bending modes and N–Fe–N bending modes. The indirect excitation of wave packets of low frequency modes via laser excited (not necessarily in the form of wave packets) higher frequency ones is rather common in many systems, including metalloporphyrins[65] and organic molecules.[66] The invariance of the oscillation period over the entire range of probe wavelengths suggests that the wave packet is created in a harmonic part of the HS surface on which it evolves, that is near its minimum. Alternatively, it is the potential surface itself which is very harmonic, but this seems unlikely.

Most notable in relation to the population mechanism of the quintet state is the fact that the rise of the quintet absorption corresponds to the decay of the ^{3}MLCT, which implies that relaxation into the $^5T_2$ state bypasses intermediate MC states. This conclusion was further confirmed in the case of $[Fe(phen)_3]^{2+}$ in acetonitrile by Tribollet *et al.*[67] who measured a $^3\text{MLCT} \rightarrow {}^5T_2$ relaxation time of 220 fs.

15.3.3 Vibrational relaxation of the HS State

A direct ^{3}MLCT to $^5T_2$ transition implies that ∼1.3 eV[27, 56], corresponding to the energy difference of the relative minima, is stored as vibrational energy in the HS state. The damping times of the wave packet represent a lower limit of its dephasing time since, as mentioned above, they also depend on the probe window. The dephasing causes the coherent (oscillatory) wave packet dynamics to turn into an incoherent kinetic regime (exponential). Given that the largest dephasing time we found is ∼800 fs, we associate the 1.1 ps decay component to the dephasing of the 130 cm^{-1} mode. Concerning the 3.4 ps decay, we associate it to the relaxation time of the (incoherently) excited Fe–N stretch mode in the quintet state. Since the ^{1,3}MLCT emission is already vibrationally cold at very early times, at least as far as the high frequency Franck–Condon modes are concerned,[57] upon crossing into the quintet state only the Fe–N stretch and the N–Fe–N chelate modes are excited, which are responsible for the bimodal relaxation regime.

The issue of vibrational energy storage and relaxation in the quintet state of Fe(II) polypyridine complexes in solution is important for the understanding of the spin photoswitching in crystals. It has mainly been studied by time-resolved resonance Raman spectroscopy.[35, 38] Recently McCusker, Mathies and co-workers used fs stimulated Raman scattering to study the vibrational relaxation in the HS state of $[Fe(tren(py)_3)]^{2+}$ in acetonitrile,[51] and reported a bimodal time evolution of the high frequency C–N stretch mode with time constants of 190 ± 50 fs and 10 ± 3 ps. A previous TA study had inferred a relaxation time of 8 ± 3 ps for $[Fe(tren(py)_3)]^{2+}$.[10] The 10 ps component was attributed to vibrational cooling, while the 190 fs component was associated with the structural change from LS to HS. Wolf *et al.*[68] reported on a sub-ps IR study of $[Fe(btpa)]^{2+}$ and $[Fe(b(bdpa))]^{2+}$ in the 1000–1100 cm^{-1} region, and found relaxation times of up to 13 ps. Thus, contrary to the case of the electronic relaxation, vibrational relaxation in the HS state depends on the complex, which is logical since the vibrational modes change. Nevertheless, the dissipation of excess vibrational energy is still not fully understood, nor is the role of the solvent clearly described. It is likely that in crystals, the vibrational cooling is slower, but the amount of energy dissipated per molecule would be sufficient to switch unexcited molecules to the HS state, simply by heating.

15.4 Ultrafast X-Ray Studies

Probing the structure of the HS state in SCO complexes using X-ray diffraction (XRD) or X-ray absorption spectroscopy (XAS) has been carried out on crystals whose HS state is long-lived and can be populated by pressure, light or temperature.[18, 34, 43, 69–72] In all the cases studied the Fe–N bond elongation from the LS to the HS state amounted to ∼0.2 Å, as a result of populating the antibonding $d(e_g)$ orbitals. The derivation of the structure of short lived HS states is not possible by quasi-steady state XRD or XAS methods, which need to be pushed into the short time domain in order to capture the short lived HS state. In recent years, picosecond XRD[19] and XAS[73–75] have been developed, which enable the probing of transient structures with the 50–100 ps resolution of synchrotrons. XAS in particular offers the advantage of being chemically selective since one tunes to the core transitions of a specific atom, and of providing information about the electronic structure of the intermediate via the pre-edge absorption bands at the K-edges (which are due to transitions from the 1*s* core orbital) in the hard X-ray range, or the edge bands at the L-edges in the soft X-ray range. In particular, the $L_{2,3}$ edges are due to transitions from the $2p_{1/2,3/2}$ core orbitals and are dipole allowed to the 3*d* valence orbitals, which are exactly those involved in the SCO process (Fig. 15.1). In addition, molecular structure can be extracted from analysis of the multiple scattering XANES (X-ray near edge absorption structure) features, and the single scattering EXAFS (extended X-ray absorption fine structure). Finally, XAS can be implemented in any type of medium, in particular in solutions, in which most of the short-lived SCO complexes have been identified.[38, 46–49]

As previously mentioned, for Fe(II) complexes with long-lived metastable HS states, quasi-static X-ray diffraction and X-ray absorption spectroscopy studies determined the Fe–N bond elongation to be ∼0.2 Å with respect to the ground state, independent of the ligands.[34] For short-lived HS states with ns and sub-ns lifetimes, one may ask if the bond elongation is also similar. Quantum-chemical calculations indeed predicted this to be the case for various Fe(II) complexes.[26–30] In order to confirm it, Khalil *et al.*[20] determined the structure of $[Fe(tren(py)_3)]^{2+}$ in acetonitrile solution, whose HS lifetime is 60 ns, using picosecond XAS,[76] and found an elongation of 0.21 ± 0.03 Å. In the case of $[Fe(bpy)_3]^{2+}$, the HS lifetime is 650 ps and with the 70 ps time resolution of the Swiss Light Source synchrotron, the transient HS structure was determined by the Lausanne group.

Figure 15.6a shows the static K-edge XAS spectrum of a 25 mM aqueous $[Fe(bpy)_3]^{2+}$complex. It is characterized by a number of XANES features, which are displayed in the inset and have already been discussed for similar ferrous polypyridine complexes.[70, 77] Suffices it to say that all have been shown in steady-state XAS studies to undergo significant changes upon light-, pressure- or temperature-induced spin-transitions.[42, 43, 70–72, 77] It is important to note that the B-band is a multiple scattering (i.e. a structural) XANES feature, as was clearly shown in ref. 70. Most of these changes have been attributed to changes of metal–ligand and intra-ligand bond distances and angles, with the Fe–N bond being the dominant contributor. Additional changes in the high energy (EXAFS) region were also clearly observed, which likewise point to a significant Fe–N bond change.[42, 43, 72, 78, 79]

Figure 15.6b shows the transient difference XAS spectrum measured 50 ps after laser excitation. All the aforementioned changes are indeed occurring as a result of laser excitation and transient population of the $^5T_2$ state. That the latter is responsible for these changes is confirmed by the inset showing the temporal evolution of the absorption changes at the B-feature (7126 eV), which maps the lifetime of the quintet state measured by optical laser spectroscopy.[56] The structural analysis of the excited state based on the transient XANES and EXAFS spectra deliver the same Fe–N bond elongation of $\Delta R_{Fe-N} = 0.20$ Å. Thus, along with the results of Khalil *et al.* for a complex with a 60 ns HS lifetime,[20] and of the literature for metastable HS states,[34] our result on the shortest-lived HS complex shows that the Fe–N bond elongation in the HS state is indeed nearly the same for all Fe(II) polypypridine complexes. This is therefore not the parameter that controls the quintet

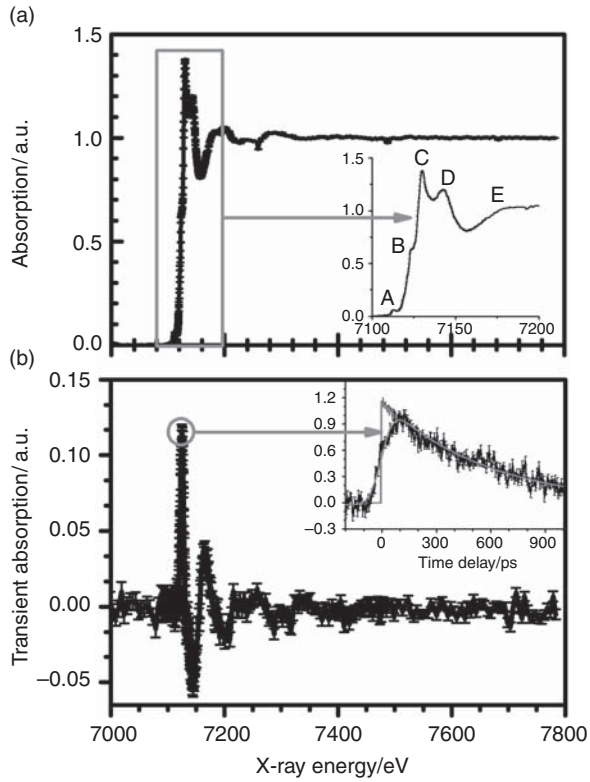

Figure 15.6 *(a) K-edge X-ray absorption spectrum of the ground LS state of aqueous $[Fe(bpy)_3]^{2+}$. The inset zooms into the first 100 eV of the spectrum and displays the details of the absorption edge and the nearest-lying XANES resonances (labelled from A–D). The onset of the EXAFS range is represented by the E feature. (b) Transient difference spectrum, recorded 50 ps after the laser pump pulse, with its error bars. The inset displays the kinetics traces of the transient X-ray absorption signal recorded at 7126 eV (feature B – black line) as compared to the optical signal recorded in transmission at 523 nm (grey line).*

state lifetime. Rather, the adiabatic energy and the couplings between low spin and high spin state are the crucial parameters. Indeed, of all Fe(II) SCO complexes, $[Fe(bpy)_3]^{2+}$ has the highest lying quintet state.

In order to follow in real-time the change of structure from the ^{1}MLCT state to the $^5T_2$ state, we carried out a femtosecond XANES study of $[Fe(bpy)_3]^{2+}$ exploiting the fact that the multiple-scattering B-feature is sensitive to the Fe–N bond elongation, as seen in Figure 15.6b. This sensitivity to the Fe–N bond length is supported by simulations based on multiple scattering theories.[23] Thus, because the $^{1,3}T$ states all lie at an intermediate distance between the LS and HS states (Fig. 15.1)**,** and considering that they have no known spectroscopic signatures in the optical domain, one should in principle be able to identify them in the XANES spectrum by the amplitude of the B-feature if they are at all involved in the relaxation cascade. However, this necessitates tuneable femtosecond hard X-ray pulses since the population time of the quintet state is ∼130 fs (see Section 15.3.1). Using the pulses generated by the slicing scheme at the Swiss Light Source,[80] the Lausanne team carried out an optical pump/X-ray probe experiment following the evolution of the B-feature as a function of pump-probe delay. Figure 15.7 presents the time scan obtained at the B-feature (7.122 keV) showing that the signal stabilizes from about 300 fs up to the scan limit of 10 ps (see inset), which is evidence

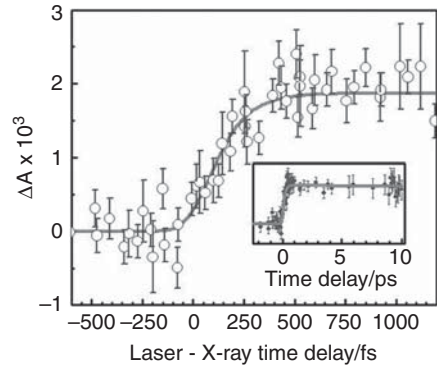

Figure 15.7 *Femtosecond XANES results: time scan of the signal (circles) at the B-feature (Fig. 15.6), as a function of laser pump/X-ray probe time delay after excitation of aqueous* $[Fe(bpy)_3]^{2+}$ *at 400 nm. The inset shows a long time scan up to 10 ps time delay. The solid line is the simulated signal assuming a simple 4-step kinetic model* $^1A_1 \rightarrow {}^1MLCT \rightarrow {}^3MLCT \rightarrow {}^5T$ *to describe the spin conversion process. See ref. 23 for details.*

that the system is already in the HS state. Further evidence is the energy scan at 300 fs, which reproduces the transient spectrum at 50 ps time resolution (see Fig. 2 of ref. 23). The fit in Figure 15.7 shows that the quintet state is reached in 150 ± 50 fs, confirming the above result using broadband UV TA (Section 15.3.2), which implies that the ultrafast spin conversion is a simple three-step ^{1}MLCT–^{3}MLCT–$^5T_2$ cascade that bypasses the intermediate $^{1,3}T$ states.

Later, Huse *et al.* carried out ps[24] and fs[25] studies at the Fe $L_{2,3}$ edges of the ultrafast SCO of $[Fe(tren(py)_3)]^{2+}$ in solution. These experiments are particularly challenging as the Fe L edges lie in the 700 eV region, which means that one needs to work under vacuum. They achieved this *tour de force* using liquid cells equipped with soft X-ray transparent silicon nitride windows. While their results confirmed the scenario already presented in refs 15 and 23, they do represent a precedent in demonstrating the possibility of carrying out ultrafast XAS at the Fe L-edges, which provides more details on the electronic structure than the K-edge, which is more adequate for molecular structure. Another tool that delivers much insight into the electronic structure of species is X-ray emission spectroscopy (XES). Indeed, while XAS probe the density of unoccupied states, XES probes that of unoccupied states and is a valuable tool to extract information about the spin structure of the system. In a proof of principle experiment, Vanko *et al.*[81] recorded, with a resolution of 70 ps, the changes of the $K_{\alpha 1}$ XES spectrum of Fe upon photoexcitation of aqueous $[Fe(bpy)_3]^{2+}$.

15.5 Summary and Outlook

The combination of cutting-edge ultrafast optical and X-ray spectroscopic tools allows one to retrieve the complete photocycle of Fe^{II} SCO complexes in solution. Here we focused on the model compound $[Fe(bpy)_3]^{2+}$ in water, and the various steps involved in its photocycle are shown in Figure 15.8. The first event is an ultrafast sequence of IVR/IC in the ^{1}MLCT state and ISC to the ^{3}MLCT state, followed by a second ISC into the quintet state, leaving the latter with a significant excess of vibrational energy. The HS undergoes vibrational relaxation in a bimodal fashion, which we believe to be due to the relaxation of the Fe–N elongation mode and of the bending and chelate modes of bpy. The latter are coherently excited by the impulsive Fe–N bond elongation, giving rise to wave packet oscillations. Finally, the return to the ground state occurs on a much slower timescale of 650 ps. The main conclusion here is that population of the HS

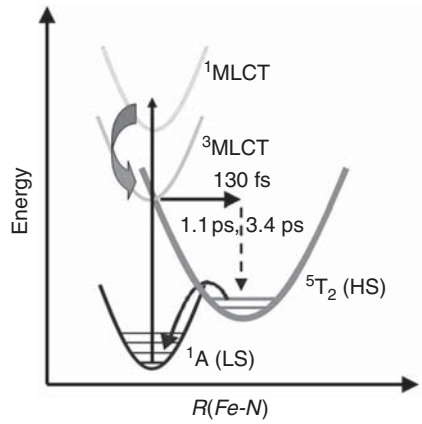

Figure 15.8 *The full photocycle of the ultrafast light-induced spin-crossover process in $[Fe(bpy)_3]^{2+}$ in water at room temperature.*

state proceeds directly and on an ultrafast timescale (<200 fs) from the ^{1,3}MLCT manifold, bypassing the intermediate MC states. This mechanism is most probably identical in the other Fe(II) SCO complexes so far studied by ultrafast spectroscopy.[25, 51, 67]

The direct population of the HS state from the MLCT manifold resolves a number of issues that were debated in the literature. The exclusion of the $^{1,3}T$ states solves the problem of multiple ultrafast ISC steps, which have to occur on an ultrafast timescale between states that are quasi-parallel with respect to the Fe–N coordinate (i.e. with poor vibrational overlap, Fig. 15.1). In addition, the unit quantum efficiency of the SCO process from the ^{1}MLCT state into the quintet state now makes sense in the context of excluding any leakage back to the ground state through the bypassing of the $^{1,3}T$ states. It is also interesting to note that the $^1A_1 \rightarrow {}^{1,3}\text{MLCT} \rightarrow {}^5T_2$ mechanism we unravel is quite close to the mechanism proposed by Hendrickson and co-workers in 1993, except that they did not include the ^{3}MLCT state in their cascade.[47] However, the timescale of the $^1\text{MLCT} \rightarrow {}^3\text{MLCT}$ ISC,[56] the presence of a weak ^{3}MLCT absorption on the red edge of the ^{1}MLCT absorption, and the fact that the latter has an absorption coefficient that is one order of magnitude smaller than that of organic dyes with pure singlet states, suggest that the singlet and triplet MLCT states are strongly mixed. Surprisingly, the initially proposed relaxation mechanism was later replaced by a mechanism invoking the intermediate $^{1,3}T$ states that would be strongly mixed. The latter statement does not seem to be supported by the low temperature steady-state spectroscopic studies,[6] which point to a clear classification of the LF states according to their spin quantum number.

The proposed mechanism is also in line with the steady-state spectroscopic studies at cryogenic temperatures, which showed that excitation into the $^{1,3}T$ states leads to population of the $^5T_2$ state with a quantum efficiency of ~80%.[6] However, for excitation of the ^{1}MLCT state, the relaxation process to the HS state was reported to occur with 100% efficiency at both 10 K[82] and at room temperature.[45, 52] This high efficiency suggested a direct decay of the ^{1}MLCT state to the HS state, since including the intermediate $^{1,3}T$ states can only decrease the conversion efficiency. The timescale of ~150 fs for the $\text{MLCT} \rightarrow {}^5T_2$ conversion corresponds to about two oscillations of the Fe–N stretch vibration,[33] suggesting a non-Born–Oppenheimer process. Excitation of the MC states also populates the HS state with high efficiency,[6] but the pathways and their timescales still need to be determined.

Given the common electronic, structural and ultrafast kinetic properties of Fe(II) complexes, we believe that the ultrafast spin relaxation in $[Fe(bpy)_3]^{2+}$ is representative for the entire family of such complexes.

However, the vibrational relaxation kinetics differs from complex to complex, just as the well-studied HS to LS relaxation back to the ground state.

There are, however, still some outstanding issues that need to be solved in order to fully describe the ultrafast light-induced SCO process. First, it is still not clear why the MC quintet state is exclusively populated from the MLCT manifold of states, while MC triplet and singlet states are avoided although they cross the MLCT states near the same point as the quintet state. Theoretical work has attempted to answer this question. Chang *et al*.[83] proposed a cascade with an intermediate step involving a ^{5}MLCT state, instead of the direct conversion of the ^{3}MLCT to the final HS state. This means that the complete SCO takes place in the MLCT manifold on a very short timescale. Once the system is in the quintet spin coupling, there is no way back through the triplet and singlet coupled ligand field states. The weakness of this model is that experimental evidence for a ^{5}MLCT state is lacking. Indeed, the absorption spectrum of the metastable HS state has been recorded in low temperature crystals and it shows only the red-infrared band due to the ^5T–^5E transition between MC states,[6] and the UV band similar to that reported in Figure 15.4. de Graaf and Sousa[31] also rule out a role for the ^{5}MLCT state, as their estimated energy places it too high to account for the cascade.

The understanding of the exact mechanism leading to population of the HS state is not just of relevance for simple Fe(II) polypyridine complexes. It has been reported with similar timescales in mono- and homodinuclear and heterodinuclear six-coordinate $[\text{Fe-M(PMK)}_3]^{2+}$ (M = Fe, Zn; PMK= bis-bidentate ligand 2-(pyridylmethyl)ketazine) complexes.[84] In addition, ultrafast spin $\Delta S = 2$ changes have been reported in metalloporphyrins[85] upon excitation of the Soret band and quite remarkably, they occur on the same timescale (∼150 fs) as reported here.

Secondly, the excitation of the ^{1,3}MC states has also been found to populate the ^5T state with high efficiency (∼80%).[6] This is quite surprising as these states also cross the ground state potential surface and in some case they share the same spin with it. It therefore seems surprising that the nonradiative channels funnel the population preferentially into the HS state. This behaviour needs to be clarified by time-resolved studies that would selectively excite the ^{1,3}MC states.

Lastly, there is growing evidence of a solvent effect on the electronic structure of the dissolved molecules,[86] in addition to its effects on their relaxation dynamics.[87–89] For the ultrafast SCO process, only one theoretical study has so far addressed this issue specifically,[32] showing the involvement of the solvent in the process of HS state formation. A recent ultrafast experimental study on a diplatinum complex by van der Veen *et al*.[90] showed a clear solvent dependence of the ISC rate.

Future studies should address the above questions with a multiple-method approach as presented here. With the advent of novel tools such as ultrafast soft X-ray absorption spectroscopy at the L-edge, time-resolved X-ray emission spectroscopy and ultrafast photoelectron spectroscopy of liquid jets,[91] there is no doubt that new insight will be reached.

Acknowledgements

This work was funded by the Swiss National Science Foundation (FNRS), via contracts 110464, 107956, 620-066145 and 105239, and by the Staatssekretariat für Bildung und Forschungcontract COST D35 C06.0016. Great thanks to all my co-workers who contributed to this work: W. Gawelda, C. Consani, M. Prémont-Schwarz, V.-T. Pham, A. ElNahhas, R. M. van der Veen, C. Bressler, C.J. Milne, T. Penfold and F. van Mourik. We also acknowledge the great help of the team at the MicroXAS beamline of the Swiss Light Source (PSI, Villigen): S. Johnson, P. Beaud, D. Grolimund, C. N. Borca, G. Ingold, R. Abela. Thanks also to M. Benfatto (Rome) for theoretical support and A. Hauser (Geneva) for many fruitful discussions and for samples.

References

1. Gütlich, P., Goodwin, H. A. (2004) Spin crossover – an overall perspective, in: Gütlich, P., Goodwin, H. A. (Eds) Spin Crossover in Transition Metal Compounds I. Top. Curr. Chem., 233: 1–47.
2. McGarvey, J. J., Lawthers, I., Heremans, K., Toftlund, H. (1984) Spin-state relaxation dynamics in iron(II) complexes: solvent on the activation and reaction and volumes for the $^1A \rightleftharpoons {}^5T$ interconversion. J. Chem. Soc. Chem. Commun., 1575–1576.
3. Lawthers, I., McGarvey, J. J. (1984) Spin-state relaxation dynamics in iron(III) complexes: photochemical perturbation of the $^2T \rightleftharpoons {}^6A$ spin equilibrium by pulsed-laser irradiation in the ligand-to-metal charge-transfer absorption band. J. Am. Chem. Soc., 106: 4280–4282.
4. Decurtins, S., Gutlich, P., Hasselbach, K. M., Hauser, A., Spiering, H. (1985) Light-induced excited-spin-state trapping in iron(II) spin-crossover systems. Optical spectroscopic and magnetic susceptibility study. Inorg. Chem., 24: 2174–2178.
5. Hauser, A. (2004) Ligand field theoretical considerations, in: Gütlich, P., Goodwin, H. A. (Eds) Spin Crossover in Transition Metal Compounds I. Top. Curr. Chem., 233: 49–58.
6. Hauser, A. (2004) Light-induced spin crossover and the high-spin→low-spin relaxation, in: Gütlich, P., Goodwin, H. A. (Eds) Spin Crossover in Transition Metal Compounds II. Top. Curr. Chem., 234: 155–198.
7. Létard, J.-F., Guionneau, P., Goux-Capes, L. (2004) Towards spin crossover applications, in: Gütlich, P., Goodwin, H. A. (Eds) Spin Crossover in Transition Metal Compounds III. Top. Curr. Chem., 235: 221–249.
8. Bousseksou, A., Molnár, G., Salmon, L., Nicolazzi, W. (2011) Molecular spin crossover phenomenon: recent achievements and prospects. Chem. Soc. Rev., 40: 3313–3335.
9. Ferrere, S., Gregg, B. A. (1998) Photosensitization of TiO_2 by $[Fe^{II}(2,2'\text{-bipyridine-4,4'-dicarboxylic acid})_2(CN)_2]$: band selective electron injection from ultra-short-lived excited states. J. Am. Chem. Soc., 120: 843–844.
10. Monat, J. E., McCusker, J. K. (2000) Femtosecond excited-state dynamics of an iron(ii) polypyridyl solar cell sensitizer model. J. Am. Chem. Soc., 122: 4092–4097.
11. Ferrere, S. (2002) New photosensitizers based upon $[Fe^{II}(L)_2(CN)_2]$ and $[Fe^{II}L_3]$, where L is substituted 2,2′-bipyridine. Inorg. Chim. Acta, 329: 79–92.
12. Xia, H.-L., Ardo, S., Sarjeant, A. A. N., Huang, S. X., Meyer, G. J. (2009) Photodriven spin change of Fe(II) benzimidazole compounds anchored to nanocrystalline TiO_2 thin films. Langmuir, 25: 13641–13652.
13. Grätzel, M. (2009) Recent advances in sensitized mesoscopic solar cells. Acc. Chem. Res., 42: 1788–1798.
14. Juban, E. A., Smeigh, A. L., Monat, J. E., McCusker, J. K. (2006) Ultrafast dynamics of ligand-field excited states. Coord. Chem. Rev., 250: 1783–1791.
15. Cannizzo, A., Milne, C. J., Consani, C., Gawelda, W., Bressler, C., van Mourik, F., Chergui, M. (2010) Light-induced spin crossover in Fe(II)-based complexes: the full photocycle unraveled by ultrafast optical and X-ray spectroscopies. Coord. Chem. Rev., 254: 2677–2686.
16. Glijer, D., Hébert, J., Trzop, E., Collet, E., Toupet, L., Cailleau, H., Matouzenko, G. S., Lazar, H. Z., Létard, J.-F., Koshihara, S., Buron-Le Cointe, M. (2008) Photoinduced phenomena and structural analysis associated with the spin-state switching in the $[Fe^{II}(DPEA)(NCS)_2]$ complex. Phys. Rev. B, 78: 134112/1–134112/9.
17. Moisan, N., Servol, M., Lorenc, M., Tissot, A., Boillot, M.-L., Cailleau, H., Koshihara, S., Collet, E. (2008) Towards ultrafast spin-state switching in the solid state. C. R. Chimie, 11: 1235–1240.
18. Ichiyanagi, K., Hébert, J., Toupet, L., Cailleau, H., Guionneau, P., Létard, J.-F., Collet, E. (2006) Nature and mechanism of the photoinduced spin transition in $[Fe(PM\text{-}BiA)_2(NCS)_2]$. Phys. Rev. B, 73: 060408/1–060408/4.
19. Cailleau, H., Lorenc, M., Guérin, L., Servol, M., Collet, E., Buron-Le Cointe, M. (2010) Structural dynamics of photoinduced molecular switching in the solid state. Acta Cryst. Sect. A, 66: 189–197.
20. Khalil, M., Marcus, M. A., Smeigh, A. L., McCusker, J. K., Chong, H. H. W., Schoenlein, R. W. (2006) Picosecond X-ray absorption spectroscopy of a photoinduced iron(ii) spin crossover reaction in solution. J. Phys. Chem. A, 110: 38–44.
21. Gawelda, W., Pham, V. T., Benfatto, M., Zaushitsyn, Y., Kaiser, M., Grolimund, D., Johnson, S. L., Abela, R., Hauser, A., Bressler, C., Chergui, M. (2007) Structural determination of a short-lived excited iron(II) complex by picosecond x-ray absorption spectroscopy. Phys. Rev. Lett., 98: 057401/1–057401/4.

22. Gawelda, W., Pham, V. T., Van der Veen, R. M., Grolimund, D., Abela, R., Chergui, M., Bressler, C. (2009) Structural analysis of ultrafast extended X-ray absorption fine structure with subpicometer spatial resolution: application to spin crossover complexes J. Chem. Phys., 130: 124520/1–124520/9.
23. Bressler, C., Milne, C., Pham, V. T., El Nahhas, A., van der Veen, R. M., Gawelda, W., Johnson, S., Beaud, P., Grolimund, D., Kaiser, M., Borca, C. N., Ingold, G., Abela, R., Chergui, M. (2009) Femtosecond XANES study of the light-induced spin crossover dynamics in an iron(II) complex. Science, 323: 489–492.
24. Huse, N., Kim, T. K., Jamula, L., McCusker, J. K., de Groot, F. M. F., Schoenlein, R. W. (2010) Photo-induced spin-state conversion in solvated transition metal complexes probed via time-resolved soft x-ray spectroscopy. J. Am. Chem. Soc., 132: 6809–6816.
25. Huse, N., Cho, H., Hong, K., Jamula, L., de Groot, F. M. F., Kim, T. K., McCusker, J. K., Schoenlein, R. W. (2011) Femtosecond soft X-ray spectroscopy of solvated transition-metal complexes: deciphering the interplay of electronic and structural dynamics. J. Phys. Chem. Lett., 2: 880–884.
26. Rodriguez, J. H. (2005) Ground- and excited-state electronic structure of an iron-containing molecular spin photoswitch. J. Chem. Phys., 123: 094709/1–094709/6.
27. Daku, L. M. L., Vargas, A., Hauser, A., Fouqueau, A., Casida, M. E. (2005) Assessment of density functionals for the high-spin/low-spin energy difference in the low-spin iron(II) tris(2,2′-bipyridine) complex. ChemPhysChem, 6: 1393–1410.
28. Ordejon, B., de Graaf, C., Sousa, C. (2008) Light-induced excited-state spin trapping in tetrazole-based spin crossover systems. J. Am. Chem. Soc., 130: 13961–13968.
29. Suaud, N., Bonnet, M. L., Boilleau, C., Labeguerie, P., Guihery, N. (2009) Light-induced excited spin state trapping: ab initio study of the physics at the molecular level. J. Am. Chem. Soc., 131: 715–722.
30. de Graaf, C., Sousa, C. (2010) Study of the light-induced spin crossover process of the $[Fe^{II}(bpy)_3]^{2+}$ complex. Chem. Eur. J. 16: 4550–4556.
31. De Graaf, C., Sousa, C. (2011) On the role of the metal-to-ligand charge transfer states in the light-induced spin crossover in $Fe^{II}(bpy)_3$. Int. J. Quantum Chem., 111: 3385–3393.
32. Daku, L. M. L., Hauser, A. (2010) Ab initio molecular dynamics study of an aqueous solution of $[Fe(bpy)_3](Cl)_2$ in the low-spin and in the high-spin states. J. Phys. Chem. Lett., 1: 1830–1835.
33. Tuchagues, J. P., Bousseksou, A., Molnar, G., McGarvey, J. J., Varret, F. (2004) The role of molecular vibrations in the spin crossover phenomenon, in: Gütlich, P., Goodwin, H. A. (Eds) Spin Crossover in Transition Metal Compounds III. Top. Curr. Chem., 235: 85–103.
34. Guionneau, P., Marchivie, M., Bravic, G., Létard, J.-F., Chasseau, D. (2004) Structural aspects of spin crossover. Example of the $[Fe^{II}L_n(NCS)_2]$ complexes, in: Gütlich, P., Goodwin, H. A. (Eds) Spin Crossover in Transition Metal Compounds II. Top. Curr. Chem., 234: 97–128.
35. Brady, C., Callaghan, P. L., Ciunik, Z., Coates, C. G., Døssing, A., Hazell, A., McGarvey, J. J., Schenker, S., Toftlund, H., Trautwein, A. X., Winkler, H., Wolny, J. A. (2004) Molecular structure and vibrational spectra of spin-crossover complexes in solution and colloidal media: resonance Raman and time-resolved resonance Raman studies. Inorg. Chem., 43: 4289–4299.
36. Huby, N., Guérin, L., Collet, E., Toupet, L., Ameline, J. C., Cailleau, H., Roisnel, T., Tayagaki, T., Tanaka, K. (2004) Photoinduced spin transition probed by x-ray diffraction. Phys. Rev. B, 69: 020101/1–020101/4.
37. Lorenc, M., Hébert, J., Moisan, N., Trzop, E., Servol, M., Buron-Le Cointe, M., Cailleau, H., Boillot, M.-L., Pontecorvo, E., Wulff, M., Koshihara, S., Collet, E. (2009) Successive dynamical steps of photoinduced switching of a molecular Fe(III) spin-crossover material by time-resolved X-ray diffraction. Phys. Rev. Lett., 103: 028301/1–028301/4.
38. Brady, C., McGarvey, J. J., McCusker, J. K., Toftlund, H., Hendrickson, D. N. (2004) Time-resolved relaxation studies of spin crossover systems in solution, in: Gütlich, P., Goodwin, H. A. (Eds) Spin Crossover in Transition Metal Compounds III. Top. Curr. Chem., 235: 1–22.
39. Daku, L. M. L., Vargas, A., Hauser, A. (2008) Private communication.
40. Ando, H., Nakao, Y., Sato, H., Sakaki, S. J. (2007) Theoretical study of low-spin, high-spin, and intermediate-spin states of $[Fe^{III}(pap)_2]^+$ (pap = N-2-pyridylmethylidene-2-hydroxyphenylaminato). Mechanism of light-induced excited spin state trapping. Phys. Chem. A, 111: 5515–5522.

41. Figgis, B. N., Hitchman, M. A. (2000) Ligand Field Theory and its Applications. Wiley-VCH, New York, p. 376.
42. Okamoto, K., Nagai, K., Miyawaki, J., Kondoh, H., Ohta, T. (2003) XAFS study on the photoinduced spin transition of $[Fe(2\text{-pic})_3]Cl_2 \cdot C_2H_5OH$. Chem. Phys. Lett., 371: 707–712.
43. Oyanagi, H., Tayagaki, T., Tanaka, K. (2004) Photo-induced phase transitions probed by X-ray absorption spectroscopy: Fe(II) spin crossover complex. J. Phys. Chem. Solids., 65: 1485–1489.
44. Ronayne, K. L., Paulsen, H., Höfer, A., Dennis, A. C., Wolny, J. A., Chumakov, A. I., Schünemann, V., Winkler, H., Spiering, H., Bousseksou, A., Gütlich, P., Trautwein, A. X., McGarvey, J. J. (2006) Vibrational spectrum of the spin crossover complex $[Fe(phen)_2(NCS)_2]$ studied by IR and Raman spectroscopy, nuclear inelastic scattering and DFT calculations. Phys. Chem. Chem. Phys., 8: 4685–4693.
45. Creutz, C., Chou, M., Netzel, T. L., Okumura, M., Sutin, N. (1980) Lifetimes, spectra, and quenching of the excited states of polypyridine complexes of iron(II), ruthenium(II), and osmium(II). J. Am. Chem. Soc., 102: 1309–1319.
46. McCusker, J. K., Toftlund, H., Rheingold, A. L., Hendrickson, D. N. (1993) Ligand conformational changes affecting $^5T_2 \rightarrow {}^1A_1$ intersystem crossing in a ferrous complex. J. Am. Chem. Soc., 115: 1797–1804.
47. McCusker, J. K., Walda, K. N., Dunn, R. C., Simon, J. D., Magde, D., Hendrickson, D. N. (1992) Sub-picosecond $\Delta S = 2$ intersystem crossing in low-spin ferrous complexes. J. Am. Chem. Soc., 114: 6919–6920.
48. McCusker, J. K., Walda, K. N., Dunn, R. C., Simon, J. D., Magde, D., Hendrickson, D. N. (1993) Subpicosecond $^1MLCT \rightarrow {}^5T_2$ intersystem crossing of low-spin polypyridyl ferrous complexes. J. Am. Chem. Soc., 115: 298–307.
49. McCusker, J. K., Rheingold, A. L., Hendrickson, D. N. (1996) Variable-temperature studies of laser-initiated $^5T_2 \rightarrow {}^1A_1$ intersystem crossing in spin-crossover complexes: empirical correlations between activation parameters and ligand structure in a series of polypyridyl ferrous complexes. Inorg. Chem., 35:, 2100–2112.
50. McCusker, J. K. (2003) Femtosecond absorption spectroscopy of transition metal charge-transfer complexes. Acc. Chem. Res., 36:, 876–887.
51. Smeigh, A. L., Creelman, M., Mathies, R. A., McCusker, J. K. (2008) Femtosecond time-resolved optical and raman spectroscopy of photoinduced spin crossover: temporal resolution of low-to-high spin optical switching. J. Am. Chem. Soc., 130: 14105–14107.
52. Bergkamp, M. A., Chang, C. K., Netzel, T. L. (1983) Quantum yield determinations for subnanosecond-lived excited states and photoproducts: applications to inorganic complexes and photosynthetic models. J. Phys. Chem., 87: 4441–4446.
53. Enachescu, C., Oetliker, U., Hauser, A. (2002) Photoexcitation in the spin-crossover compound $[Fe(pic)_3]Cl_2 \cdot EtOH$ (pic = 2-picolylamine). J. Phys. Chem. B, 106: 9540–9545.
54. Hauser, A. (1991) Intersystem crossing in the $[Fe(ptz)_6](BF_4)_2$ spin crossover system (ptz=1-propyltetrazole). J. Chem. Phys., 94: 2741–2748.
55. Cannizzo, A., van Mourik, F., Gawelda, W., Zgrablic, G., Bressler, C., Chergui, M. (2006) Broadband femtosecond fluorescence spectroscopy of $[Ru(bpy)_3]^{2+}$. Angew. Chem. Int. Ed., 45: 3174–3176.
56. Gawelda, W., Cannizzo, A., Pham, V. T., van Mourik, F., Bressler, C., Chergui, M. (2007) Ultrafast Nonadiabatic Dynamics of $[Fe^{II}(bpy)_3]^{2+}$ in Solution. J. Am. Chem. Soc., 129: 8199–8206.
57. Bräm, O., Messina, F., El-Zohry, A., Cannizzo, A., Chergui, M. (2012) Polychromatic femtosecond fluorescence studies of metal–polypyridine complexes in solution. Chem. Phys., 393: 51–57.
58. Braterman, P. S., Song, J. I., Peacock, R. D. (1992) Electronic absorption spectra of the iron(II) complexes of 2,2′-bipyridine, 2,2′-bipyrimidine, 1,10-phenanthroline, and 2,2′:6′,2″-terpyridine and their reduction products. Inorg. Chem., 31: 555–559.
59. Tarnovsky, A., Gawelda, W., Johnson, M., Bressler, C., Chergui, M. (2006) Photexcitation of aqueous ruthenium(II)-tris-(2,2′-bipyridine) with high-intensity femtosecond laser pulses. J. Phys. Chem. B, 110: 26497–26505.
60. Gawelda, W., Johnson, M., de Groot, F. M. F, Abela, R., Bressler, C., Chergui, M. (2006) Electronic and molecular structure of photoexcited $[Ru^{II}(bpy)_3]^{2+}$ probed by picosecond x-ray absorption spectroscopy. J. Am. Chem. Soc., 128: 5001–5009.
61. Chang, H. R., Mccusker, J. K., Toftlund, H., Wilson, S. R., Trautwein, A. X., Winkler, H., Hendrickson, D. N. (1990) [Tetrakis(2-pyridylmethyl)ethylenediamine]iron(II) perchlorate, the first rapidly interconverting ferrous spin-crossover complex. J. Am. Chem. Soc., 112: 6814–6827.
62. Xie, C. L., Hendrickson, D. N. (1987) Mechanism of spin-state interconversion in ferrous spin-crossover complexes: direct evidence for quantum mechanical tunneling. J. Am. Chem. Soc., 109: 6981–6988.

63. Consani, C., Prémont-Schwarz, M., Elnahhas, A., Bressler, C., van Mourik, F., Cannizzo, A., Chergui, M. (2009) Vibrational coherences and relaxation in the high-spin state of aqueous $[Fe^{II}(bpy)_3]^{2+}$. Angew. Chem. Int. Ed., 48: 7184–7187.
64. Alexander, B. D., Dines, T. J., Longhurst, R. W. (2008) DFT calculations of the structures and vibrational spectra of the $[Fe(bpy)_3]^{2+}$ and $[Ru(bpy)_3]^{2+}$ complexes. Chem. Phys., 352: 19–27.
65. Rosca, F., Kumar, A. T. N., Ionascu, D., Ye, X., Demidov, A. A., Sjodin, T., Wharton, D., Barrick, D., Sligar, S. G., Yonetani, T., Champion, P. M. (2002) Investigations of anharmonic low-frequency oscillations in heme proteins. J. Phys. Chem. A, 106: 3540–3552.
66. Zgrablic, G., Haacke, S., Chergui, M. (2007) Vibrational coherences of the protonated Schiff base of all-trans retinal in solution. Chem. Phys.,338: 168–174.
67. Tribollet, J., Galle, G., Jonusauskas, G., Deldicque, D., Tondusson, M., Létard, J.-F., Freysz, E. (2011) Transient absorption spectroscopy of the iron(II) $[Fe(phen)_3]^{2+}$ complex: Study of the non-radiative relaxation of an isolated iron(II) complex. Chem. Phys. Lett., 513: 42–47.
68. Wolf, M. M. N., Groß, R., Schumann, C., Wolny, J. A., Schünemann, V., Døssing, A., Paulsen, H., McGarvey, J. J., Diller, R. (2008) Sub-picosecond time resolved infrared spectroscopy of high-spin state formation in Fe(II) spin crossover complexes. Phys. Chem. Chem. Phys., 10: 4264–4273.
69. Hannay, C., HubinFranskin, M. J., Grandjean, F., Briois, V., Itié, J.-P., Polian, A., Trofimenko, S., Long, G. J. (1997) X-ray absorption spectroscopic study of the temperature and pressure dependence of the electronic spin states in several iron(II) and cobalt(ii) tris(pyrazolyl)borate complexes. Inorg. Chem., 36: 5580–5588.
70. Briois, V., Sainctavit, P., Long, G. J., Grandjean, F. (2001) Importance of photoelectron multiple scattering in the iron K-edge X-ray absorption spectra of spin-crossover complexes: full multiple scattering calculations for several iron(II) trispyrazolylborate and trispyrazolylmethane complexes. Inorg. Chem., 40: 912–918.
71. Boillot, M.-L., Zarembowitch, J., Itié, J.-P., Polian, A., Bourdet, E., Haasnoot, J. G. (2002) Pressure-induced spin-state crossovers at room temperature in iron(II) complexes: comparative analysis; a XANES investigation of some new transitions. New J. Chem., 26: 313–322.
72. Oyanagi, H., Tayagaki, T., Tanaka, K. (2006) Synchrotron radiation study of photo-induced spin-crossover transitions: microscopic origin of nonlinear phase transition. J. Luminesc., 119: 361–369.
73. Bressler, C., Abela, R., Chergui, M. (2008) Exploiting EXAFS and XANES for time-resolved molecular structures in liquids. Z. Kristallogr. 223: 307–321.
74. Bressler, C., Chergui, M. (2010) Molecular structural dynamics probed by ultrafast X-ray absorption spectroscopy. Ann. Rev. Phys. Chem., 61: 263–282.
75. Chergui, M. (2010) Picosecond and femtosecond X-ray absorption spectroscopy of molecular systems. Acta Cryst. Sect. A, 66: 229–239.
76. Saes, M., Bressler, C., van Mourik, F., Gawelda, W., Kaiser, M., Chergui, M., Bressler, C., Grolimund, D., Abela, R., Glover, T. E., Heimann, P. A., Schoenlein, R. W., Johnson, S. L., Lindenberg, A. M., Falcone, R. W. (2004) A setup for ultrafast time-resolved x-ray absorption spectroscopy. Rev. Sci. Instrum., 75: 24–30.
77. Briois, V., Moulin, C. C. D., Sainctavit, P., Brouder, C., Flank, A. M. (1995) Full multiple scattering and crystal field multiplet calculations performed on the spin transition $Fe^{II}(phen)_2(NCS)_2$ complex at the iron K and $L_{2,3}$ X-ray absorption edges. J. Am. Chem. Soc., 117: 1019–1026.
78. Yokoyama, T., Murakami, Y., Kiguchi, M., Komatsu, T., Kojima, N. (1998) Spin-crossover phase transition of a chain Fe(II) complex studied by X-ray-absorption fine-structure spectroscopy. Phys. Rev. B, 58: 14238–14244.
79. Boča, R., Vrbová, M., Werner, R., Haase, W. (2000) Spin crossover in iron(II) tris(2-(2-pyridyl)benzimidazole) complex monitored by the variable temperature EXAFS. Chem. Phys. Lett., 328: 188–196.
80. Beaud, P., Johnson, S. L., Streun, A., Abela, R., Abramsohn, D., Grolimund, D., Krasniqi, F., Schmidt, T., Schlott, V., Ingold, G. (2007) Spatiotemporal stability of a femtosecond hard–X-ray undulator source studied by control of coherent optical phonons. Phys. Rev. Lett., 99: 174801/1–174801/4.
81. Vankó, G., Glatzel, P., Pham, V. T., Abela, R., Grolimund, D., Borca, C. N., Johnson, S. L., Milne, C. J., Bressler, C. (2010) Picosecond time-resolved X-ray emission spectroscopy: ultrafast spin-state determination in an iron complex. Angew. Chem. Int. Ed., 49: 5910–5912.
82. Enachescu, C., Oetliker, U., Hauser, A. (2003) The quantum efficiency of the photo-excitation in a Fe (II) spin-crossover compound. J. Opt. Adv. Mater., 5: 267–272.

83. Chang, J., Fedro, A. J., van Veenendaal, M. (2010) Ultrafast cascading theory of intersystem crossings in transition-metal complexes. Phys. Rev. B, 82: 075124/1–075124/5.
84. Lapini, A., Foggi, P., Bussotti, L., Righini, R., Dei, A. (2008) Relaxation dynamics in three polypyridyl iron(II)-based complexes probed by nanosecond and sub-picosecond transient absorption spectroscopy. Inorg. Chim. Acta, 361: 3937–3943.
85. Champion, P. M., Rosca, F., Ionascu, D., Cao, W. X., Ye, X. (2004) Rapid timescale processes and the role of electronic surface coupling in the photolysis of diatomic ligands from heme proteins. Faraday Discuss., 127: 123–135.
86. Aziz, E. F., Rittmann-Frank, M. H., Lange, K. M., Bonhommeau, S., Chergui, M. (2010) Charge transfer to solvent identified using dark channel fluorescence-yield L-edge spectroscopy. Nature Chem., 2: 853–857.
87. Moret, M. E., Tapavicza, E., Guidoni, L., Röhrig, U. F., Sulpizi, M., Tavernelli, I., Rothlisberger, U. (2005) Quantum mechanical/molecular mechanical (QM/MM) Car-Parrinello simulations in excited states. Chimia, 59: 493–498.
88. Moret, M. E., Tavernelli, I., Rothlisberger, U. (2009) Combined QM/MM and classical molecular dynamics study of $[Ru(bpy)_3]^{2+}$ in water. J. Phys. Chem. B, 113: 7737–7744.
89. Moret, M. E., Tavernelli, I., Chergui, M., Rothlisberger, U. (2010) Electron localization dynamics in the triplet excited state of $[Ru(bpy)_3]^{2+}$ in aqueous solution. Chem. Eur. J., 16: 5889–5894.
90. van der Veen, R. M., Cannizzo, A., van Mourik, F., Vlček, A. jr., Chergui, M. (2011) Vibrational relaxation and intersystem crossing of binuclear metal complexes in solution. J. Am. Chem. Soc., 133: 305–315.
91. Link, O., Lugovoy, E., Siefermann, K., Liu, Y., Faubel, M., Abel, B. (2009) Ultrafast electronic spectroscopy for chemical analysis near liquid water interfaces: concepts and applications. Appl. Phys. A Mater. Sci. Process., 96: 117–135.